NASA MEMO 2-26-59A

NASA

MEMORANDUM

SOME FINITE DIFFERENCE SOLUTIONS OF THE LAMINAR COMPRESSIBLE BOUNDARY LAYER SHOWING THE EFFECTS OF UPSTREAM TRANSPIRATION COOLING

By John T. Howe

Ames Research Center
Moffett Field, Calif.

NATIONAL AERONAUTICS AND SPACE ADMINISTRATION
WASHINGTON
February 1959

NATIONAL AERONAUTICS AND SPACE ADMINISTRATI N

MEMORANDUM 2-26-59A

SOME FINITE DIFFERENCE SOLUTIONS OF THE LAMINAR COMPRESSIBLE BOUNDARY LAYER SHOWING THE EFFECTS OF UPSTREAM TRANSPIRATION COOLING

By John T. Howe

SUMMARY

Three numerical solutions of the partial differential equations describing the compressible laminar boundary layer are obtained by the finite difference method described in reports by I. Flügge-Lotz, D. C. Baxter, and this author. The solutions apply to steady-state supersonic flow without pressure gradient, over a cold wall and over an adiabatic wall, both having transpiration cooling upstream, and over an adiabatic wall with upstream cooling but without upstream transpiration.

It is shown that for a given upstream wall temperature, upstream transpiration cooling affords much better protection to the adiabatic solid wall than does upstream cooling without transpiration.

The results of the numerical solutions are compared with those of approximate solutions. The thermal results of the finite difference solution lie between the results of Rubesin and Inouye, and those of Libby and Pallone. When the skin-friction results of one finite difference solution are used in the thermal analysis of Rubesin and Inouye, improved agreement between the thermal results of the two methods of solution is obtained.

INTRODUCTION

Cooling problems arising from high-speed flight have stimulated interest in transpiration cooling of vehicle surfaces. Aerodynamic heating and the need for cooling are often quite localized on an aircraft, which makes it possible to restrict the porous surfaces associated with transpiration cooling to selected regions on the aircraft. Structural considerations make it desirable to limit the porous region as much as possible. A limited region of transpiration cooling may provide some thermal protection to regions downstream. References 1 and 2 have presented analytic methods for evaluating the thermal protection afforded a surface adjacent to and downstream from a transpiration-cooled region.

The results of the two analyses differ considerably because of different assumptions made in joining the flows at the interface between the porous and nonporous regions. This present report does not have to make such assumptions.

This report evaluates the thermal protection afforded in three flow conditions by finite difference solutions of the laminar compressible boundary-layer equations. The first two conditions are flow over a cooled solid wall and an adiabatic solid wall downstream from a porous transpiration-cooled region. The third condition is flow over an adiabatic wall downstream from a solid cooled region without transpiration. In all three flow conditions, the upstream wall temperatures are the same. The exterior flow conditions for all cases are $M_e = 3.0$ and $T_e = 389.99^\circ$ R. The latter is the tropopause (top of the troposphere) flight temperature (ref. 3). The results are compared with those of references 1 and 2.

The finite difference solutions of the partial differential equations were computed on an IBM-650 digital computer.

SYMBOLS

a velocity of sound, ft/sec

b_n coefficient in the $i_u\tau$ expansion, equation (A14)

c_n coefficient in the i^2 expansion, equation (A17)

c_f local skin-friction coefficient, $\frac{\tau_w}{\frac{1}{2}\rho_e u_e^2}$

c_p specific heat at constant pressure, sq ft/sec^2 $^\circ$R

c_v specific heat at constant volume, sq ft/sec^2 $^\circ$R

C_1 Chapman-Rubesin constant (ref. 4) based on upstream region wall temperature

d_n coefficient in the τ^2 expansion, equation (A12)

f_w variable proportional to blowing rate in reference 5

h local heat-transfer coefficient, $\frac{q_w}{T_w - T_{ad}}$, lb/ft sec $^\circ$R

i	enthalpy, $c_p T$, sq ft/sec^2
i^+	dimensionless enthalpy, $\frac{i}{a_t^2}$
Δi	enthalpy difference, sq ft/sec^2
k	thermal conductivity, lb/sec $^\circ$R
L	reference length, ft
M_e	Mach number at outer edge of boundary layer
m	number of mesh widths from the starting value of x, $\frac{x-x_i}{\Delta x}$
n	number of mesh widths from wall, $\frac{u}{\Delta u}$
p	static pressure, lb/sq ft
P	parameter used in computer program logic (appendix C)
ΔP	increment of P
Pr	Prandtl number, $\frac{c_p \mu}{k}$, 0.72 for air
q	local heat-transfer rate, $-kT_y = \frac{-i_u \tau}{Pr}$, lb/ft sec
Q	parameter used in computer program logic (appendix C)
R	gas constant for air, sq ft/sec^2 $^\circ$R
Re_x	Reynolds number based on properties at outer edge of the boundary layer, $\frac{u_e x \rho_e}{\mu_e}$
Re_t	Reynolds number based on stagnation properties, $\frac{a_t L \rho_t}{\mu_t}$
S	constant in the Sutherland law, $^\circ$R
St	Stanton number, $\frac{h}{\rho_e u_e c_p}$
T	absolute temperature, $^\circ$R

T_{ad}	adiabatic wall temperature computed by equation (15) of reference 5, ^{o}R
u	component of velocity parallel to the surface, ft/sec
Δu	interval between mesh points in the u direction, ft/sec
v	component of velocity perpendicular to the surface, ft/sec
x	distance coordinate measured parallel to the surface, ft
Δx	distance between mesh points in the x direction, ft
y	distance from the surface, ft
γ	ratio of specific heats, $\frac{c_p}{c_v}$
μ	coefficient of viscosity, lb sec/sq ft
ρ	mass density, lb sec^2/ft^4
τ	shear stress, μu_y, lb/sq ft
τ^+	dimensionless shear stress, $\frac{\tau\sqrt{Re_t}}{\rho_t a_t^2}$

Subscripts

ad	adiabatic wall condition
e	conditions at outer edge of the boundary layer
i	initial value of x in defining m
u,x,y	partial differentiation with respect to u,x,y
w	wall
t	isentropic stagnation conditions for flow at the outer edge of the boundary layer
n=o,1,2	successive coefficients in a power series expansion
1	conditions in the upstream region, $\frac{x}{L} \leq 1$

Superscripts

'	total differentiation with respect to x
+	dimensionless quantity used for actual computation on digital computer (see also ref. 6, eqs. (2.8) to (2.22))

METHOD OF SOLUTION

Only a brief description of the method is included here. The many details of the method can be found in references 6, 7, 8, and 9. A mathematical description of the solution is included in appendix A. The minor modifications to the computer program are presented in block diagram form in appendix C.

The laminar compressible boundary-layer equations in the Crocco form (ref. 10) are solved on a finite difference basis progressing downstream from $x/L = 1$, where initial profiles (obtained from ref. 5) of enthalpy and shear stress across the boundary layer are specified. The specific heat, c_p, is assumed constant. Although the examples presented do not involve pressure gradients, the method is not restricted to constant pressure.

Boundary conditions at the outer edge of the boundary layer and at the wall are incorporated in the solution as they occur. Because the partial differential equations (A1) and (A2) cannot be solved at the wall (i.e., $u = 0$), each wall point is treated by series expansions; that is, a series expansion of τ^2 in terms of u, in which the coefficients are determined by boundary conditions at the wall, is written through two points within the boundary layer yielding an expression from which the wall shear stress can be obtained.

Series expansions for the thermal properties are written in a similar manner. If wall temperature is specified as a boundary condition, a series expansion for $i_u\tau$ in terms of u is written through three points in the boundary layer, finally yielding an expression for the heat transfer at the wall. If, on the other hand, the heat transfer is specified as a boundary condition, either a series expansion for i or Simpson's rule is used to obtain the wall temperature.

Other features of the finite difference solution are as follows. The flow exterior to the boundary layer is specified, and is treated by the usual isentropic flow relations. The Sutherland viscosity law is used to compute the viscosity at each mesh point. The mesh width employed in the finite difference scheme is determined by the stability criteria of reference 8 such that errors tend to vanish as the numerical solution progresses.

A TEST EXAMPLE

The computation of each example in this report extended from $x/L = 1$ to $x/L = 2$ or 2500 steps downstream from the starting profiles. Previous examples (refs. 9 and 6) computed by this program have not been carried that far. For this reason, it is desirable to use the program to try to reproduce a known solution over that many steps. The test example chosen is for flow at $M_e = 3.0$ over a solid flat plate having wall temperature level $T_w/T_{ad} = 0.5$. The shear stress and enthalpy profiles used to start the finite difference solution can be found in reference 9.

The results of the finite difference solution are shown as solid lines in figure 1. An exact solution taken from reference 5 is shown by dotted lines in figure 1. In the finite difference solution, series expansions (eqs. (A13) and (A15)) operating on the given initial profiles resulted in skin-friction and heat-transfer parameters identical to those of reference 5 at the start ($x/L = 1$). At the end of 2500 steps downstream, the finite difference value for the skin-friction parameter differed by less than 1 percent from that of reference 5. Similarly, the heat-transfer parameter differed by 1 percent from that of reference 5. The solution of the finite difference equations is considered to be correct. Figure 1 indicates that this correct solution of the finite difference equations converges satisfactorily to the numerical solution of the differential equations of reference 5 in the region shown.

It should be mentioned that the linear viscosity law is used in reference 5, and the Sutherland viscosity law is used in the finite difference solution. I. E. Beckwith suggests in a private communication that these different viscosity laws are responsible for the very small differences between the two solutions in figure 1. He points out that in reference 11, which also uses the Sutherland viscosity law, the results for the same example are about 1.5 percent less than the results of reference 5.

SOLUTIONS IN A REGION DOWNSTREAM FROM A SURFACE THAT IS COOLED WITH AND WITHOUT TRANSPIRATION

Starting Profiles and Numerical Data

The initial profiles of shear stress and enthalpy used to begin the three examples of interest are obtained from the "exact" solutions of reference 5. These exact solutions of the boundary-layer differential equations are free from many of the limitations (such as low speed flow, $Pr = 1$, and use of integral or empirical methods) of other exact solutions. Profiles with transpiration correspond to those at the end of a porous upstream region of a flat plate having transverse blowing at the wall at a rate proportional to the reciprocal of the square root of the

distance from the leading edge. In particular, profiles corresponding to $f_{w_1} = -1.0$ and $f_{w_1} = 0$ (ref. 5) are used. These profiles are at a distance $x = L$ from the leading edge of the plate. In addition, the conditions

$$T_e = 389.99^\circ \text{ R}$$

$$M_e = 3.0$$

$$T_{w_1}/T_{ad_1} = 0.5 \quad \text{for} \quad f_{w_1} = -1 \text{ example}$$

$$T_{w_1}/T_{ad_1} = 0.459 \quad \text{for} \quad f_{w_1} = 0 \text{ example}$$

are chosen to determine the starting profiles. The first one is the tropopause flight temperature (ref. 3). The last three correspond to supersonic flow over a cold upstream wall. The ratios T_{w_1}/T_{ad_1} differ between the transpiration and no transpiration upstream region examples because the upstream wall temperature is specified to be the same (452.34° R) in both cases but the recovery factors in the upstream region are different. The choice of T_e influences the base of the viscosity law mostly, and for these flat plate examples probably does not restrict the applicability of the results to other conditions of temperature and pressure, provided the Mach number and ratio of wall temperature to adiabatic temperature are unchanged. Computation of an example showed that halving T_e did not change the results by more than 1 percent.

Tables I and II list the starting profiles of enthalpy and shear stress. The tables list profiles at $x/L = 1$ at the end of upstream regions having a given wall temperature, with and without transpiration, respectively. The corresponding curves are shown in figures 2 and 3. The dimensionless terminology is used in the computer program, and is explained in the section "Symbols."

Other numerical data used in the computations were

$$\gamma = 1.4$$

$$R = 1716.5 \text{ sq ft/sec}^2\ ^\circ\text{R}$$

$$c_p = 6007.8 \text{ sq ft/sec}^2\ ^\circ\text{R}$$

$$S = 216^\circ \text{ R}$$

$$Pr = 0.72$$

The Reynolds number per foot based on tropopause outer edge conditions ($p_e = 472.68$ lb/sq ft, $T_e = 389.99^\circ$ R) was 6.93×10^6.

The Examples and Results

Case 1.- The case of supersonic flow over a solid cold wall ($T_w/T_{ad_1} = 0.5$) at uniform wall temperature downstream from the porous region is shown in figure 4. It is seen in figure 4(a) that the skin-friction parameter starts at less than 20 percent of that for the no blowing case, rising to a value of less than 70 percent of that for the no blowing case in a solid length equal to the porous length. The ratio of local heat transfer with upstream transpiration cooling to local heat transfer without upstream transpiration cooling for the same wall temperature ratio ($T_w/T_{ad_1} = 0.5$) and Mach number (but necessarily different wall temperature) is shown in figure 4(b). It is seen that in a region downstream from a porous region in a length equal to the porous length, use of upstream transpiration cooling requires a local removal of heat only 22 to 76 percent of that required to maintain the specified wall temperature ratio without upstream transpiration. Figure 5 shows the heat-transfer comparison for the case in which the local heat-transfer ratio is based on the condition that the upstream region wall temperature be the same for the porous and nonporous upstream regions. The ratio of the local heat transfer, computed for this example, to that of the solid flat plate at the same Mach number, flight conditions, and wall temperature (but necessarily different T_{ad_1} and T_w/T_{ad_1}) varies from approximately 0.20 at $x/L = 1$ to 0.70 at $x/L = 2$. This is a significant reduction in local heat transfer required to maintain a given wall temperature.

Cases 2 and 3.- Figure 6 presents the results of supersonic flow over an adiabatic solid wall downstream from a fixed temperature region cooled with and without transpiration.

The skin-friction results are shown in figure 6(a). A very substantial reduction in skin friction is effected by the upstream transpiration, as would be expected.

The ratio of wall temperature to free-stream stagnation temperature in the adiabatic region is presented in figure 6(a). Because of the assumption of constant c_p, this temperature ratio is the same as the enthalpy ratio.

The two curves labeled "transpiration upstream" are results of only one example in which two different methods of computation of the wall enthalpy were used. The solid curve was computed by the series expansion, equation (A18), and the broken curve was computed by Simpson's rule, equation (A16). The use of Simpson's rule instead of the series expansion in the computation of T_w/T_t results in a small saving of computer time. However, in reference 9 it was found that the Simpson's rule solution gives poor convergence in regions not far downstream from $x/L = 1$ for some examples. The maximum difference between the two T_w/T_t solutions is approximately 1 percent, from which it can be concluded that the Simpson's rule expression yields satisfactory results for this example.

However, the convergence difficulties reported in reference 9 require that caution be exercised in the application of Simpson's rule in general. To be safe, the series expansion for T_w/T_t should be used instead of Simpson's rule.

The first point ($x/L = 1$) computed by the program is designated "end of porous wall" on the ordinate. In each case, it coincides with the exact solution corresponding to the starting profiles used. At that first point, v_w, the component of velocity perpendicular to the wall, is different from zero. At the next step ($x/L = 1.0004$), however, v_w is specified to be zero. This is a realistic physical situation. An actual discontinuity in transverse velocity at the wall will exist where the porous region joins the solid wall. A discontinuity in skin-friction and heat-transfer parameters corresponding to the specified discontinuity in the transverse velocity at the wall is evident (between the dotted line marked "end of upstream region" and the beginning of each curve) in figures 4, 5, and 6. The series expansions used in the computation of these parameters (eqs. (A13) and (A15)) show v_w to be responsible for the discontinuity. A similar discontinuity in T_w/T_t caused by specified discontinuities in both v_w and q_w is seen in figure 6. The terms involving q_w and v_w responsible for the computed discontinuity appear in the series expansion (eq. (A18)). This unrealistic situation of discontinuous wall temperature results partly from the unrealistic specification of discontinuous heat transfer. There is of course no perfect insulator; that is, q cannot be achieved discontinuously in actual flows. Conduction would smooth out the wall temperature discontinuity.

COMPARISON WITH EXISTING SOLUTIONS

The results obtained above are compared with those computed by the methods of references 1 and 2 and are shown in figures 7 and 8. The comparison is made on the basis of identical physical situations; that is, the results of each method are presented for the same flight conditions, blowing rates, and porous-wall temperature level. Before discussing these curves in detail, it is of interest to discuss the methods by which these various results were obtained.

There is little agreement in the results of the three methods. This is no doubt due to different methods of solution and to different assumptions made in joining the flows of the porous and nonporous regions. Some of the differences in the three methods of solution appear in the table below.

Features of solution	Rubesin and Inouye (ref. 1)	Libby and Pallone (ref. 2)	Finite difference
Step-by-step integration of exact boundary-layer equations			X
Polynomial solution using von Kármán integral method	X	X	
Prandtl number	1.0	1.0	0.72
Viscosity temperature law	Linear	Linear	Sutherland
Discontinuity in wall shear stress allowed	No	Yes	Yes

References 1 and 2 are polynomial-type solutions employing the von Kármán integral methods. These are by nature approximate methods in that they deal with bulk or gross properties of the boundary layer. The finite difference solution, on the other hand, deals directly with the differential equations in finite difference form and solves them in a point-to-point pattern progressing downstream from a given solution at the end of the porous region.

The assumptions made in joining the porous and nonporous flow fields differ between references 1 and 2. The present report did not have to make such assumptions. In reference 2 velocity and enthalpy profiles downstream from the porous region were determined by specifying continuous flux of mass, momentum, and energy at the interface between the porous and nonporous regions. This leads to a discontinuity in local velocity and stagnation enthalpy profiles (as well as shear stress) at that interface. On the other hand, in reference 1 a continuous wall shear stress was assumed at the interface. This seems to be an essential difference between the solutions of references 1 and 2. The finite difference solution yields discontinuities in skin friction, heat transfer, and wall temperature at the interface, as was discussed previously.

It is to be expected that these major differences in methods of solution and assumptions will lead to different results. However, no attempt has been made to establish quantitatively the influence of any detail of the different methods on the lack of agreement among the three solutions.

Figure 7 shows the skin-friction result of the finite difference solutions compared with those of references 1 and 2. The finite difference solutions of figures 4 and 6 having upstream transpiration are adjusted to correspond to the ordinate shown in figure 7 by means of the appropriate values of $\sqrt{Re_x/C_1}$. It is seen that there is little difference between the finite difference solutions for the insulated and the cold walls. As was indicated above, the skin-friction results of all three methods

of solution differ appreciably. It is seen that the initial discontinuity in the reference 2 analysis is considerably larger than that of the finite difference solutions. It should be mentioned that the curve d was obtained by computing $c_f \sqrt{Re_x/C_1}$ by the method of reference 2, and dividing the result by the standard value 0.664 (ref. 5) adjusted slightly for the appropriate values of C_1.

The wall temperature computation results of several solutions for supersonic flow ($M_e = 3.0$) over an adiabatic solid wall downstream from a cold porous region having wall temperature level $T_{w_1}/T_{ad_1} = 0.5$ and $f_{w_1} = -1$ are shown in figure 8. Curve a is obtained from the Rubesin and Inouye analysis. Curve c is the finite difference solution using the series expansion (eq. (A18)). Curve d is obtained by the Libby and Pallone solution (ref. 2). It is seen that the latter solution predicts considerably more thermal protection than does either a or c.

The thermal analysis of reference 1 depends on the skin-friction results, which differed from those of the finite difference solution. Hence, it is not surprising that the wall temperature results of the two methods differ (curves a and c, fig. 8). However, curve b in figure 8 is the result of the thermal analysis of Rubesin and Inouye when the skin-friction results of the finite difference solution were used in that analysis. The curve shows improved agreement between the wall temperature results of the two methods of solution. The mathematical details involved in the use of finite difference results in the Rubesin and Inouye analysis are presented in appendix B.

A comparison of the heat-transfer results of the finite difference solution to those of reference 1 is shown in figure 9. The analysis of reference 2 applies only to the adiabatic wall condition, and cannot be included in this comparison. Figure 9 is a plot of the ratio of local heat transfer with to that without upstream transpiration cooling at fixed flight conditions and wall temperature. Because the wall temperature is constant in this example and Pr = 1 in reference 1, Reynolds analogy as presented in reference 12 was used to obtain the Rubesin and Inouye heat-transfer curve: The Rubesin and Inouye results are observed to lie above those of the finite difference solution for the most part. This is not surprising because the same behavior was observed in the ratio of skin-friction coefficients (fig. 7) on which the heat-transfer results of reference 1 depend.

The differing results presented for three methods of solution raise an obvious question: Which of these solutions is the best representation of the physical situation? This can be answered by briefly looking again at the methods by which the results were obtained. Briefly recapitulating, the finite difference solution is a direct numerical solution of the finite difference form of the exact boundary-layer equations. Because the step width is chosen such that errors die out, the solution of the finite difference equations is considered to be correct. The convergence of the finite difference solution to that of the differential equations

appears to be satisfactory in examples where it can be checked. The physical flow is computed taking specified boundary conditions (continuous or discontinuous) into account as they occur. The resulting solution is considered to be as realistic a representation as the flow situation that was specified.

In contrast with the above, the polynomial-type solutions of references 1 and 2 are by nature approximate solutions dealing with bulk properties across the boundary layer. Patching of solutions for the porous and nonporous region necessitates making additional assumptions. Which assumptions are appropriate is not clear.

For these reasons, the finite difference solutions are considered to be more accurate than those of references 1 and 2.

CONCLUDING REMARKS

For these examples of upstream transpiration cooling, the finite difference solutions not only produce results different from those of references 1 and 2, but different conclusions as well. Where the Libby and Pallone analysis would be very optimistic about the effects of upstream transpiration cooling, and the Rubesin and Inouye analysis would be quite conservative, the finite difference solution takes a stand between these saying that the effect is quite good in a limited region as follows.

Upstream transpiration cooling affords significant thermal protection to a solid region equal in length to the porous region for the flow conditions used in the computations ($M_e = 3.0$, $T_{w_1}/T_{ad_1} = 0.5$, $f_{w_1} = -1$, tropopause flight temperature). In particular, for the example of uniform wall temperature, the upstream transpiration cooling requires removal of heat in the solid region only 20 to 70 percent of that required to maintain that wall temperature without upstream transpiration cooling.

For the case of an adiabatic wall downstream from the transpiration-cooled region, the finite difference solution for the temperature ratio (T_w/T_t) lies below that of reference 1, but considerably above that of reference 2. Improved agreement between the T_w/T_t solution of reference 1 and the finite difference solution is achieved when the skin-friction results of the latter are used in the thermal analysis of the former. It is shown by finite difference solutions that, for a fixed upstream region temperature, upstream transpiration cooling affords much better thermal protection to the adiabatic solid region downstream than does upstream cooling without transpiration.

The finite difference solutions for skin friction lie significantly below that of reference 1 and are considerably different from that of reference 2. Similarly, the finite difference solution for heat transfer lies below that of reference 1 for the most part.

Because of the methods by which the results were obtained, the finite difference solutions are considered to be more accurate than those of references 1 and 2.

As interest in more complex boundary-layer flows grows, finite difference solutions will probably assume the major burden of boundary-layer computations; for example, axisymmetric boundary-layer flows with variable Euler number can be computed by the finite difference scheme.

Ames Research Center
National Aeronautics and Space Administration
Moffett Field, Calif., Nov. 26, 1958

APPENDIX A

MATHEMATICAL DESCRIPTION OF THE SOLUTION

Basic equations.- A basic description of the solution is included here. A detailed description is found in references 6, 7, 8, and 9.

The steady-state, two-dimensional, boundary-layer flow of a compressible fluid with variable properties can be described by the Crocco form of the boundary-layer equations. These are

$$\tau^2\tau_{uu}+\mu p_e'\tau_u+[u(\rho\mu)_x-\mu_u p_e']\tau = u\rho\mu\tau_x \tag{A1}$$

$$\frac{1-Pr}{Pr}\, i_u\tau\tau_u + \frac{i_{uu}+Pr}{Pr}\,\tau^2+\mu p_e'(i_u+u) = u\rho\mu i_x \tag{A2}$$

In the examples computed in this report, p_e' was zero. However, the computer program is not limited to examples having no pressure gradient.

The equation of state of a perfect gas and the Sutherland viscosity law are used and are, respectively,

$$p = p_e = \rho RT = \frac{\gamma-1}{\gamma}\,\rho i \tag{A3}$$

$$\frac{\mu}{\mu_t} = \left(\frac{i}{i_t}\right)^{1.5}\frac{i_t+c_pS}{i+c_pS} \tag{A4}$$

The latter assumes constant specific heat. A power law approximation[1] for the viscosity, which when differentiated is used for the computation of the term $u(\rho\mu)_x$ in the solution of equation (A1), is

$$\frac{\mu}{\mu_t} = \left(\frac{i}{i_t}\right)^{0.76} \tag{A5}$$

One of the equations used to obtain coefficients in series expansions at the wall is the momentum equation before v is eliminated by use of the continuity equation, that is

$$\rho u u_x\frac{\mu}{\tau} + \rho v = -\frac{\mu p_e'}{\tau} + \tau_u \tag{A6}$$

---

[1]The accuracy of the approximation has been investigated in reference 8 and appears satisfactory.

Boundary conditions.- The boundary conditions at the outer edge of the boundary layer are

$$\tau_e = 0 \tag{A7}$$

$$i_e = i_t - \frac{u_e^2}{2} \tag{A8}$$

At the wall, the boundary conditions are

$$\tau = \tau_w \tag{A9}$$

and if the wall temperature is specified,

$$i_w = i_w(x) \tag{A10}$$

or conversely if the heat-transfer rate is specified,

$$q_w = - \frac{i_{uw}\tau_w}{Pr} \tag{A11}$$

Series expansions near the wall.- The square of the shear stress is expanded in the series

$$\tau^2 = d_0+d_1u+d_2u^2+d_3u^3 \tag{A12}$$

which is written for the first two points out from the wall described by $u = n\Delta u$, where $n = 1$ and 2. The coefficient d_3 is eliminated from the resulting equations, and the remaining coefficients are determined from boundary and compatibility conditions, as described in reference 6. The resulting equation for the shear stress at the wall point $x/L = 1+m\Delta x/L$ is (for $p_e' = 0$)

$$\tau_w = - \frac{6}{7} \Delta u\rho_w v_w \pm \sqrt{\frac{8}{49} (\Delta u\rho_w v_w)^2 + \frac{8}{7} \tau_{m,1}^2 - \frac{1}{7} \tau_{m,2}^2} \tag{A13}$$

If i_w (eq. (A10)) is specified, a series expansion useful in determining the heat transfer at the wall is

$$i_u\tau = b_0+b_1u+b_2u^2+b_3u^3+b_4u^4 \tag{A14}$$

This equation is written through the three points $n = 1, 2, 3$ out from the wall at which $u = \Delta u, 2\Delta u$, and $3\Delta u$, respectively, all at an x location $x/L = 1+m\Delta x/L$. Both b_3 and b_4 are eliminated from the

resulting three equations. The remaining coefficients are determined as before. The resulting equation for i_{uw} in the absence of pressure gradient is

$$i_{uw} = \tau_w \frac{\left[108(i_u\tau)_{m,1}-27(i_u\tau)_{m,2}+4(i_u\tau)_{m,3}\right]}{85\tau_w^2+6\Delta u Pr\rho_w v_w\left[11\tau_w+3\Delta u(Pr-1)\rho_w v_w\right]} +$$

$$\frac{6\Delta u Pr\tau_w\left[11\tau_w+3\Delta u(Pr+1)\rho_w v_w\right] - 18\Delta u^2 Pr\mu_w i_{xw}}{85\tau_w^2+6\Delta u Pr\rho_w v_w\left[11\tau_w+3\Delta u(Pr-1)\rho_w v_w\right]} \qquad (A15)$$

If heat transfer is specified by equation (A11), the wall temperature (or enthalpy) is computed by either of two methods. The first is Simpson's rule which becomes (ref. 8):

$$i_w = \frac{1}{2}(i_{m,1}-i_{m,3})+i_{m,2}-i_{uw}\Delta u \qquad (A16)$$

The second is a series expansion for i^2 as follows.

$$i^2 = c_0+c_1u+c_2u^2+c_3u^3+c_4u^4 \qquad (A17)$$

This equation is treated in the same way as equation (A14), the coefficients being determined by boundary and compatibility conditions. The result is

$$i_w = \frac{1}{85}\left(108i_{m,1}-27i_{m,2}+4i_{m,3}+66\frac{Prq\Delta u}{\tau_w} + 18Pr\Delta u^2\left\{1+\frac{q}{\tau_w}\left[\frac{\rho_w v_w}{\tau_w}(Pr-1)-\frac{\mu_w p_e'}{\tau_w^2}\right]\right\}\right) \qquad (A18)$$

In reference 9, the Simpson's rule method was found to result in poor convergence, which made it necessary to use the series expansion to obtain i_w.

Equations (A1) and (A2) are solved at every boundary-layer mesh point as described in reference 8. Equations (A13) and (A15), (A16), or (A18) are solved at every wall point. In this manner, the solution progresses downstream.

APPENDIX B

THE FINITE DIFFERENCE SOLUTION AND THE RUBESIN AND INOUYE THERMAL ANALYSIS

In the section comparing finite difference results with those of existing solutions, the use of finite difference skin-friction results in the thermal analysis of reference 1 was discussed. The mathematical details are as follows. A quantity used in reference 1 is

$$s(x) = \frac{\rho}{\rho_w'} \left(\frac{\partial u'}{\partial y'}\right)_{x'} = \frac{T_w}{T_e} \left(\frac{\tau_w}{\mu_w}\right) \tag{B1}$$

The middle term is in the terminology of reference 1, and $s(x)$ is the quantity defined in that reference. Also $\sigma(\xi)$ from equation (A83) of reference 1 becomes

$$\sigma(\xi) = \frac{\delta_o}{u_\infty} s(x) = \frac{\delta_o}{u_\infty} \frac{T_w \tau_w}{T_\infty \mu_w} \tag{B2}$$

The subscripts e and ∞ are interchangeable. Assuming that

$$\frac{T_w}{T_\infty} = C_1 \frac{\mu_w}{\mu_\infty} \tag{B3}$$

(where C_1 is the Chapman-Rubesin constant (ref. 4) written for the porous section), leads to

$$\sigma(\xi) = \frac{\delta_o}{u_\infty} \frac{C_1}{\mu_\infty} \tau_w \tag{B4}$$

Requiring that $\sigma(1) = 0.325$ (ref. 1) and using values from the finite difference solution, one may determine $\sigma(\xi)$ from equation (B4). This makes possible the integration of equations (A83) and (A92) of reference 1, yielding the wall enthalpy distribution shown in curve b of figure 8.

APPENDIX C

COMPUTER PROGRAM MODIFICATIONS

The computer program described in block form in figure 11, reference 8, and modified by figures A-1 and A-2 of reference 6 was modified again in several ways to facilitate computations of the present examples.

Because v_w was zero for $x/L > 1$, but different from zero for $x/L = 1$ in the present examples, the obvious change was to set $v_w = 0$ after the computation of the points at $m = 0$ was complete. This was done in the part of the computation shown in sketch (a).

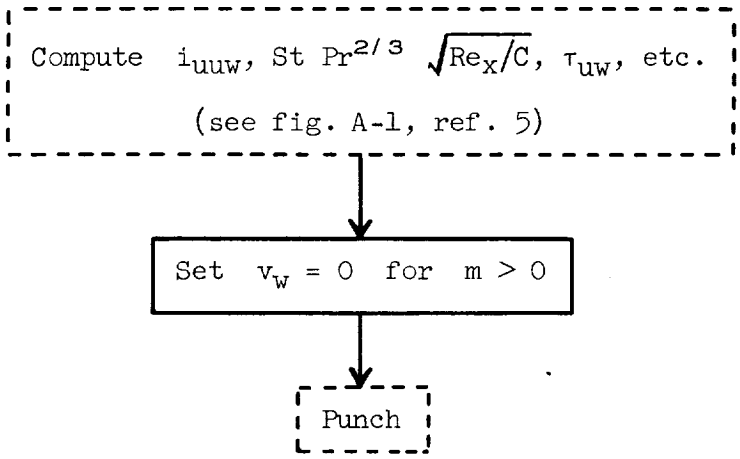

Sketch (a)

Because the examples were longer than those previously computed by this program, the output was modified to read out results of profiles and wall points of stations in which m was a given multiple of 8. This was accomplished by means of specified parameters P, ΔP, and Q in the subroutine of sketch (b). Sample values of these quantities used for punching every thirty-second downstream station are $\Delta P = 32$, and $Q = 30.8$, where the initial value of P is 31.9.

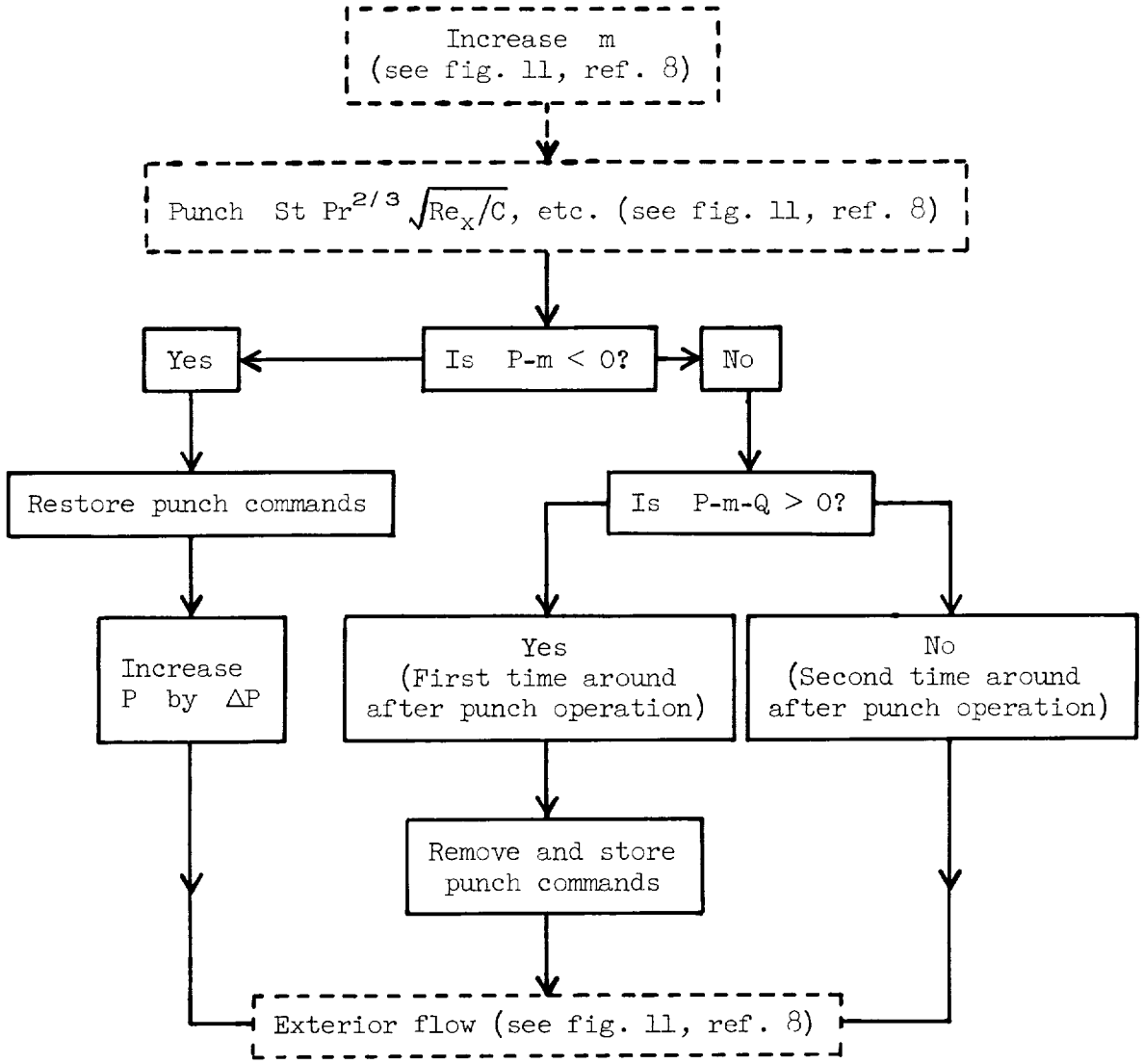

Sketch (b)

The insulated wall examples required program modifications before entrance to the exterior flow routine (i.e., at the end of the modifications of sketch (b)). These can be described best by one block of commands which, after m has been increased to 1, proceeds to

1. Compute $i_o - i_e$ in the exterior routine.

2. Set v_w, i_{uw}, q, and τ_{uuw} equal zero, in the wall point routine.

3. Compute i_w by either the series expansion or Simpson's rule in the wall point routine.

4. Compute the recovery factor in the wall point routine.

5. Skip this entire block after the program has been modified once.

These modifications to the computation scheme discussed in references 6 and 8 describe the program used to compute the examples of this report.

REFERENCES

1. Rubesin, Morris W., and Inouye, Mamoru: A Theoretical Study of the Effect of Upstream Transpiration Cooling on the Heat-Transfer and Skin-Friction Characteristics of a Compressible, Laminar Boundary Layer. NACA TN 3969, 1957.

2. Libby, Paul A., and Pallone, Adrian: A Method for Analyzing the Heat Insulating Properties of the Laminar Compressible Boundary Layer. Jour. Aero. Sci., vol. 21, no. 12, Dec. 1954, pp. 825-834.

3. Standard Atmosphere - Tables and Data for Altitudes to 65,800 Feet. NACA Rep. 1235, 1955. (Supersedes NACA TN 3182 and Rep. 218)

4. Chapman, Dean R., and Rubesin, Morris W.: Temperature and Velocity Profiles in the Compressible Laminar Boundary Layer With Arbitrary Distribution of Surface Temperature. Jour. Aero. Sci., vol. 16, no. 9, Sept. 1949, pp. 547-565.

5. Low, George M.: The Compressible Laminar Boundary Layer With Fluid Injection. NACA TN 3404, 1955.

6. Flügge-Lotz, Irmgard, and Howe, John T.: The Solution of Compressible Laminar Boundary Layer Problems By a Finite Difference Method. Part 3. The Influence of Suction or Blowing at the Wall. Tech. Rep. No. 111, ARDC Contract AF 18(600)-1488, Div. of Eng. Mech., Stanford Univ., Oct. 15, 1957.

7. Flügge-Lotz, Irmgard: The Computation of the Laminar Compressible Boundary Layer. ARDC Contract AF 18(600)-586, Proj. No. R-352-30-7, Dept. of Mech. Eng., Stanford Univ., June 1954. (Also available as: A Difference Method for the Computation of the Laminar Compressible Boundary Layer, 50 Jahre Grenzschichtforschung, Publ. Fr. Vieweg und Sohn, Braunchweig, 1955, p. 393)

8. Flügge-Lotz, Irmgard, and Baxter, Donald C.: The Solution of Compressible Laminar Boundary Layer Problems By a Finite Difference Method. Part 1. Description of the Method. Tech. Rep. No. 103, ARDC Contract AF 18(600)-1488, Div. of Eng. Mech., Stanford Univ., Sept. 30, 1956. (Also available as AFOSR-TN-56-544)

9. Baxter, Donald C., and Flügge-Lotz, Irmgard: The Solution of Compressible Laminar Boundary Layer Problems By a Finite Difference Method. Part 2. Further Discussion of the Method and Presentation of Examples. Tech. Rep. No. 110, ARDC Contract AF 18(600)-1488, Div. of Eng. Mech., Stanford Univ., Oct. 15, 1957.

10. Crocco, L.: Lo strato limite laminare nei gas, Monografie Scientifiche di Aeronautica No. 3, Associazione Culturale Aeronautica, Roma, Dic. 1946. (Trans. North American Aviation Aerophysics Lab. Rep. CF-1038, July 1948)

11. Van Driest, E. R.: Investigation of Laminar Boundary Layer in Compressible Fluids Using the Crocco Method. NACA TN 2597, 1952.

12. Schlichting, Hermann: Boundary Layer Theory. McGraw-Hill Book Co., Inc., 1955, p. 257.

TABLE I.- STARTING PROFILES FOR $M_e = 3.0$, $T_{w_1}/T_{ad_1} = 0.5$, $f_{w_1} = -1.0$, $T_e = 389.99^\circ$ R, AND $T_{w_1} = 452.34^\circ$ R

u/u_e	i^+	τ^+
0	1.0356050	0.0158900
.05	1.1006470	.0269720
.10	1.1531480	.0376120
.15	1.1968560	.0475810
.20	1.2310290	.0567680
.25	1.2587460	.0650710
.30	1.2798800	.0722150
.35	1.2947780	.0787510
.40	1.3037270	.0839720
.45	1.3065330	.0874830
.50	1.3035180	.0906380
.55	1.2950950	.0920020
.60	1.2810580	.0919220
.65	1.2608000	.0901340
.70	1.2343670	.0864770
.75	1.2021270	.0808910
.80	1.1633110	.0729990
.85	1.1169350	.0623030
.90	1.0617830	.0481770
.95	.9948670	.0292160
1.00	.8928550	.0000000

TABLE II.- STARTING PROFILES FOR $M_e = 3.0$, $T_{w_1}/T_{ad_1} = 0.459$, $f_{w_1} = 0$, $T_e = 389.99^\circ$ R, AND $T_{w_1} = 452.34^\circ$ R

u/u_e	i^+	τ^+
0	1.0356050	0.1487940
.05	1.0860114	.1487687
.10	1.1313143	.1486469
.15	1.1714895	.1483728
.20	1.2064998	.1478896
.25	1.2340550	.1469696
.30	1.2563106	.1456360
.35	1.2733546	.1438292
.40	1.2850720	.1414685
.45	1.2921466	.1383408
.50	1.2896725	.1343205
.55	1.2834143	.1294052
.60	1.2714197	.1234532
.65	1.2534401	.1162937
.70	1.2292588	.1077263
.75	1.1985191	.0975240
.80	1.1600998	.0854255
.85	1.1161789	.0710042
.90	1.0619288	.0534711
.95	.9952259	.0315010
1.00	.8928550	.0000000

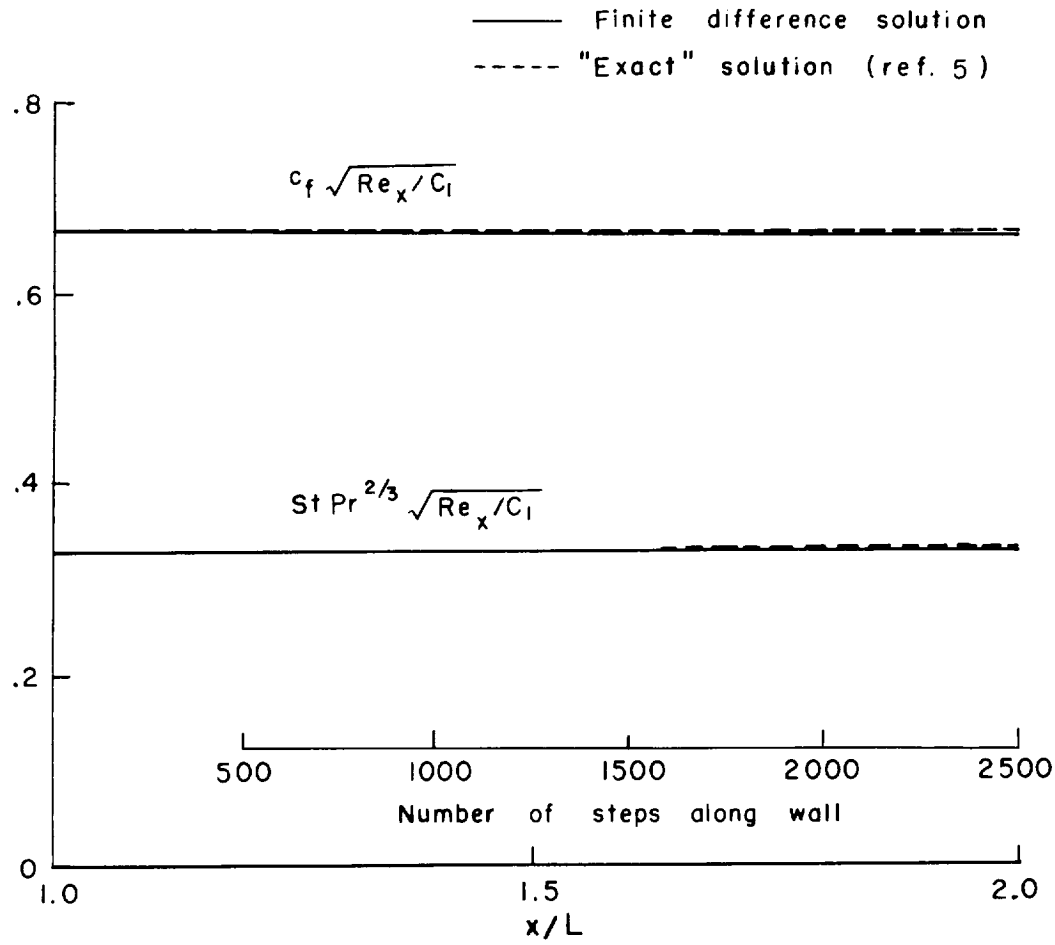

Figure 1.- Flat plate solution without upstream transpiration cooling; M_e=3.0, T_w/T_{ad}=0.5, f_w=0, tropopause flight temperature.

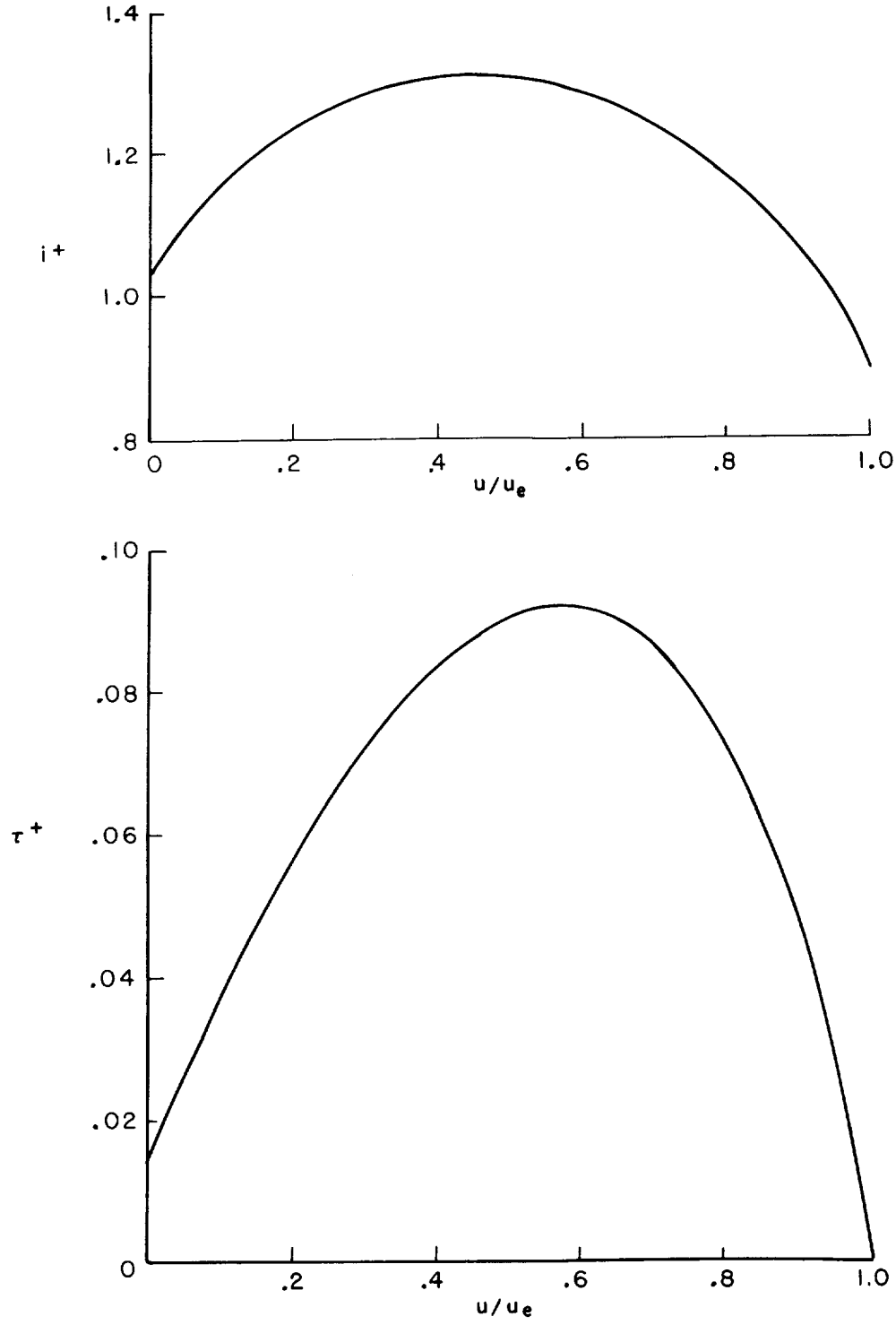

Figure 2.- Flat plate enthalpy and shear stress starting profiles for transpiration cooling; M =3.0, T_{w_1}/T_{ad_1}=0.5, f_{w_1}=-1, T_e=389.99° R, T_{w_1}=452.34° R.

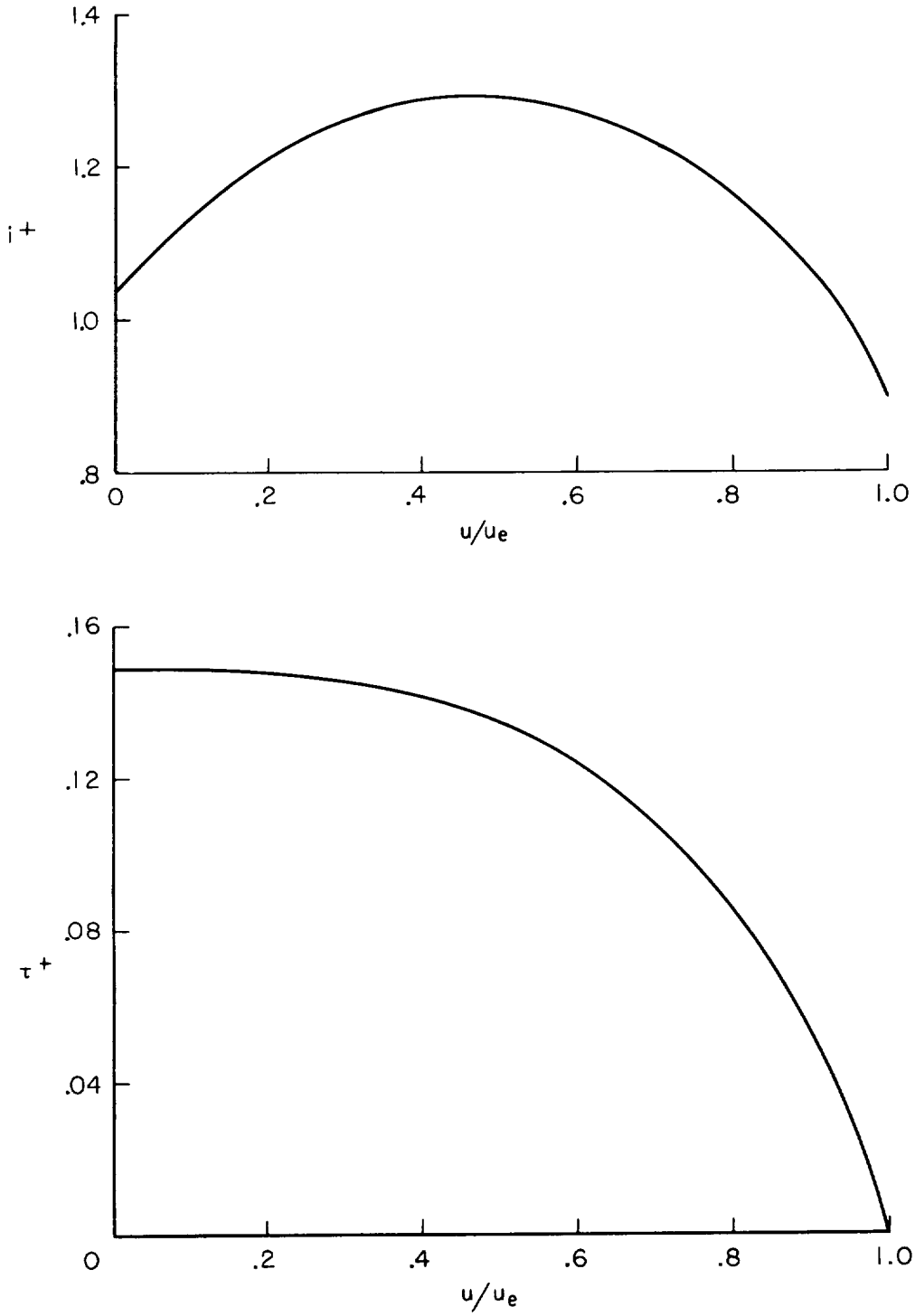

Figure 3.- Flat plate enthalpy and shear stress starting profiles for cooling without transpiration; $M_e=3.0$, $T_{w_1}/T_{ad_1}=0.459$, $F_{w_1}=0$, $T_e=389.99^{\circ}$ R, $T_{w_1}=452.34^{\circ}$ R.

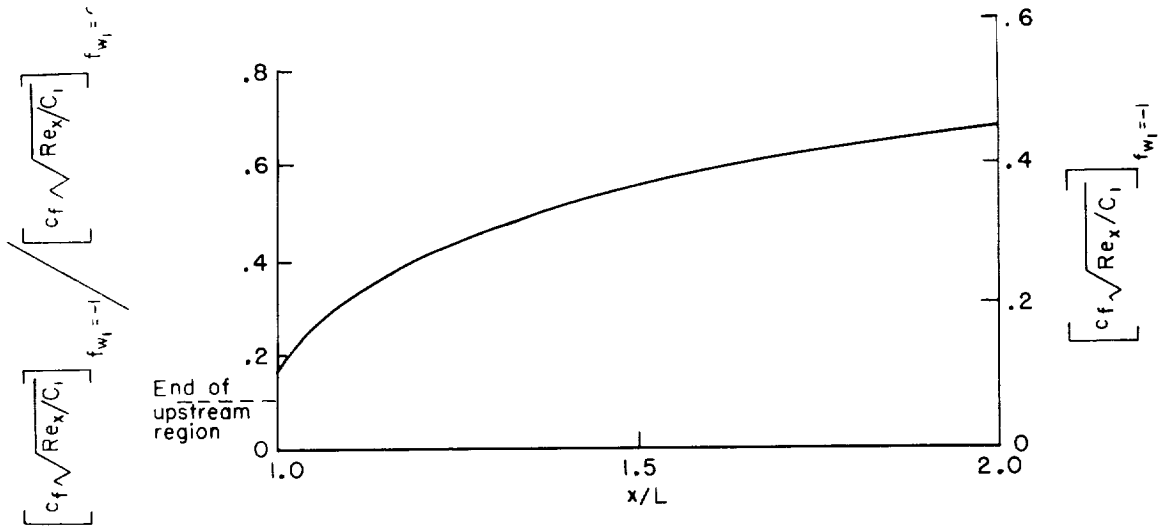

(a) Skin-friction results.

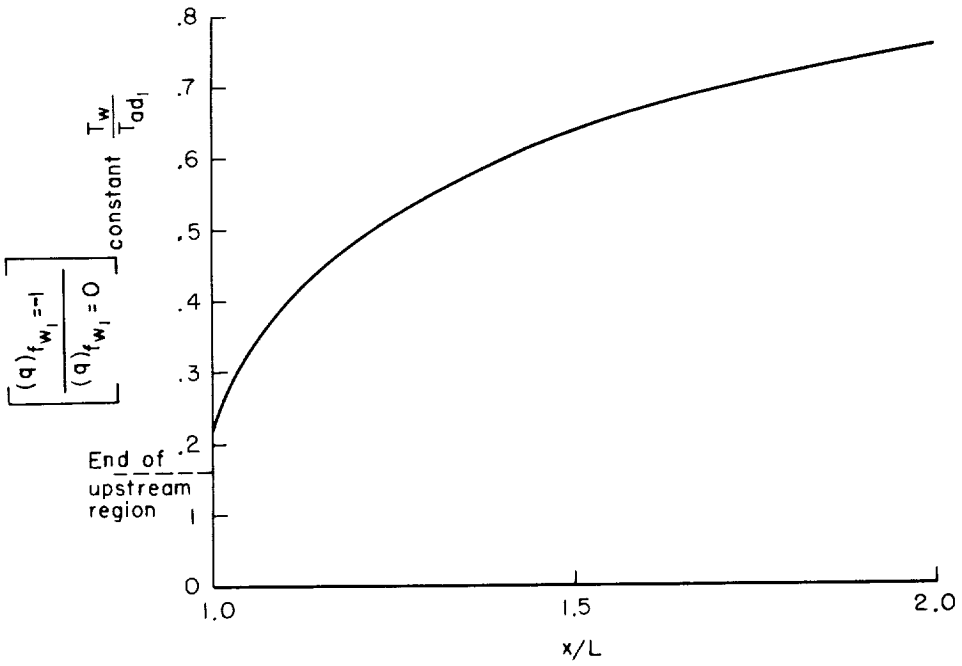

(b) Heat-transfer results.

Figure 4.- Supersonic flow over cold wall at uniform temperature downstream from transpiration cooled region; $M_e=3.0$, $T_w/T_{ad_1}=0.5$, tropopause flight temperature.

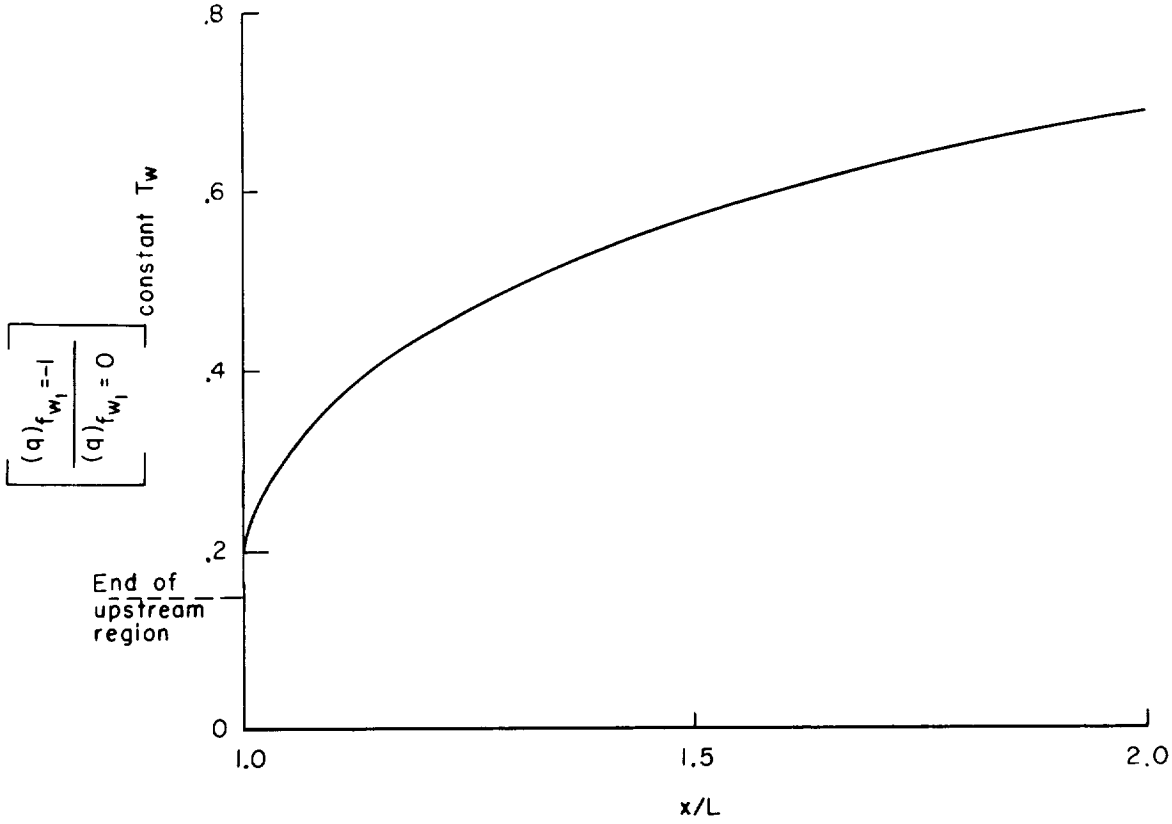

Figure 5.- Ratio of local heat transfer with to that without upstream transpiration cooling at fixed flight temperature and wall temperature; $M_e=3.0$, $T_w/T_{ad_1}=0.5$ for plate with porous upstream region, $T_w/T_{ad_1}=0.459$ for plate with solid upstream region, $T_w=452.34^{\circ}$ R for both plates, tropopause flight temperature.

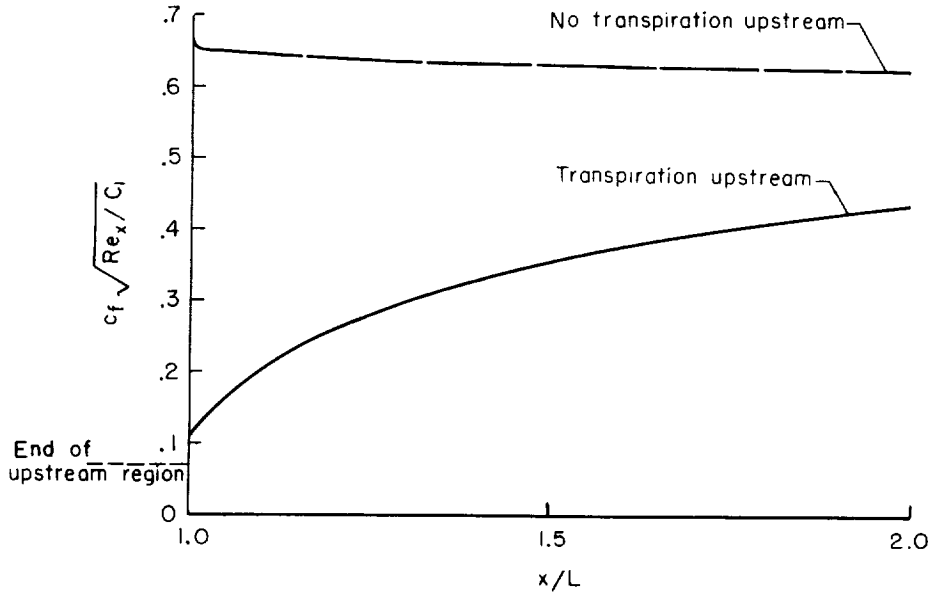

(a) Skin-friction results.

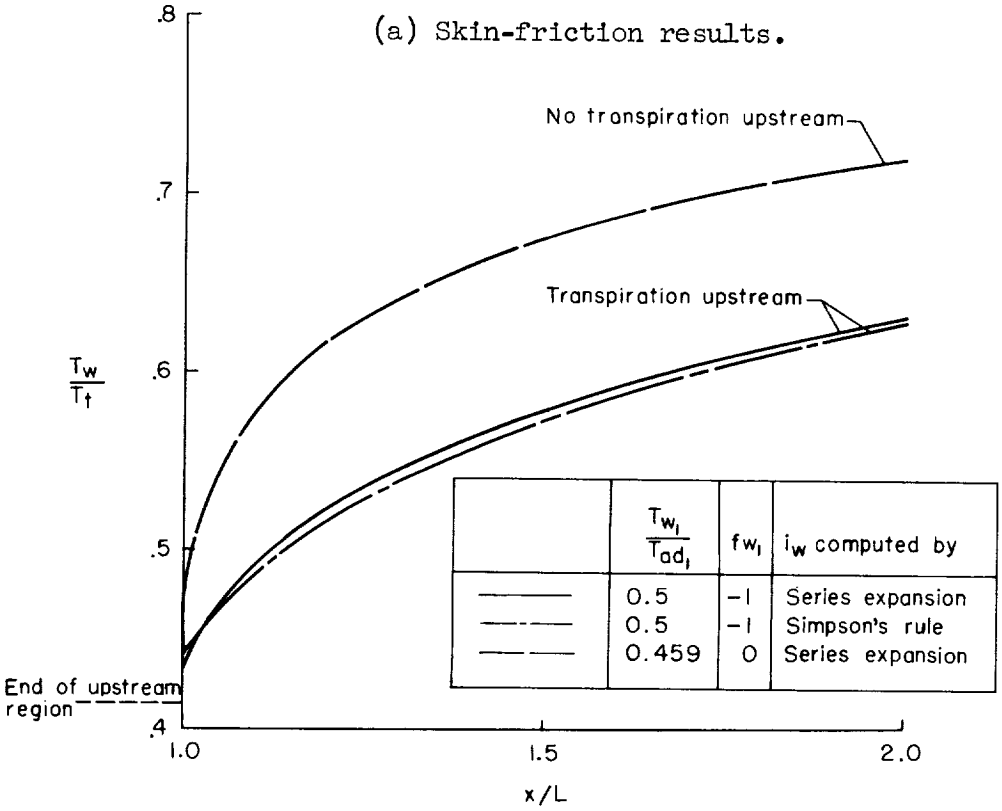

(b) Wall temperature results.

Figure 6.- Supersonic flow over adiabatic wall downstream from region at fixed temperature cooled with and without transpiration; M_e=3.0, T_{w_1}=452.34° R, tropopause flight temperature.

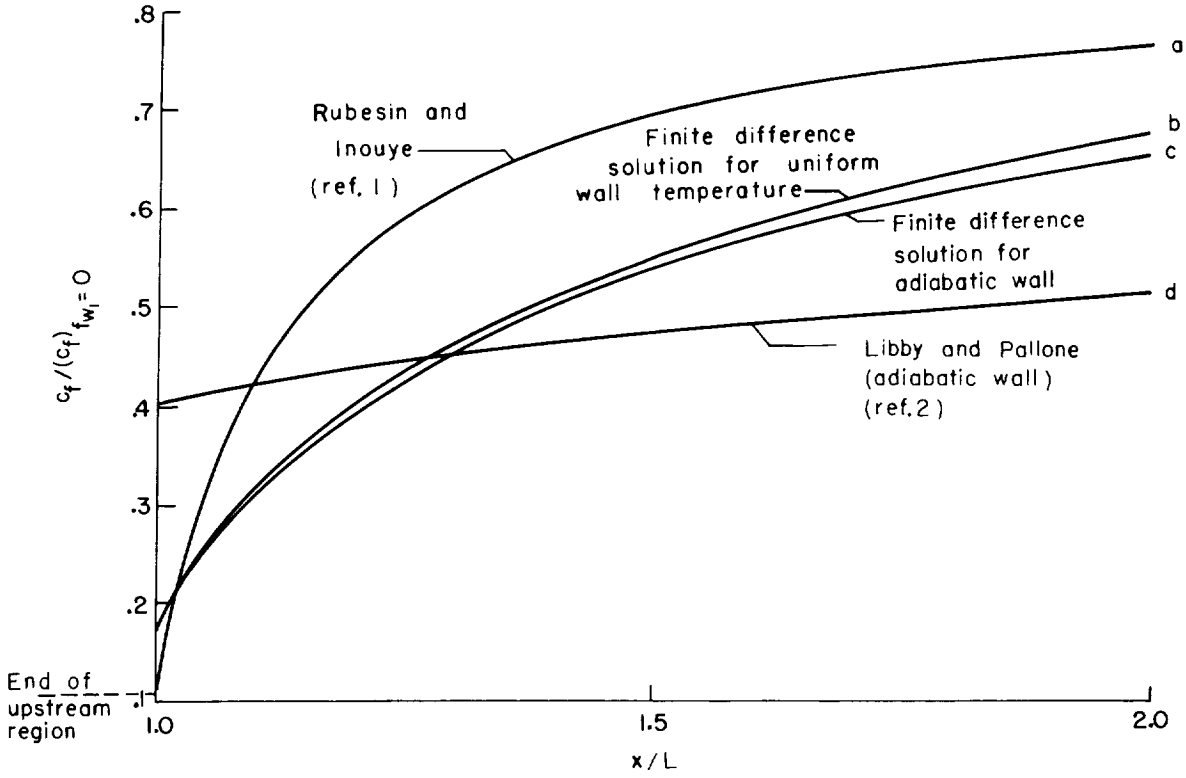

Figure 7.- Comparison of skin-friction results; $M_e=3.0$, $T_{w_1}/T_{ad_1}=0.5$, $f_{w_1}=-1$, tropopause flight temperature.

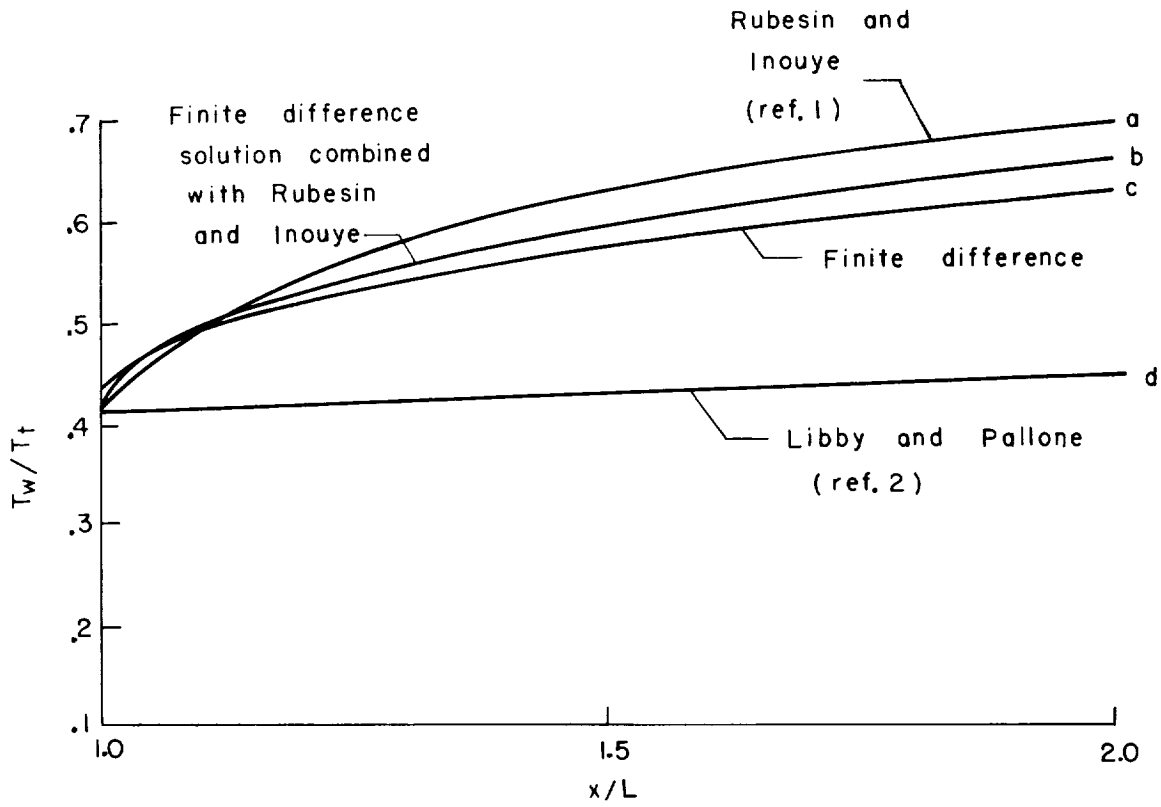

Figure 8.- Comparison of thermal results for adiabatic wall; M_e=3.0, T_{w_1}/T_{ad_1}=0.5, f_{w_1}=-1, tropopause flight temperature.

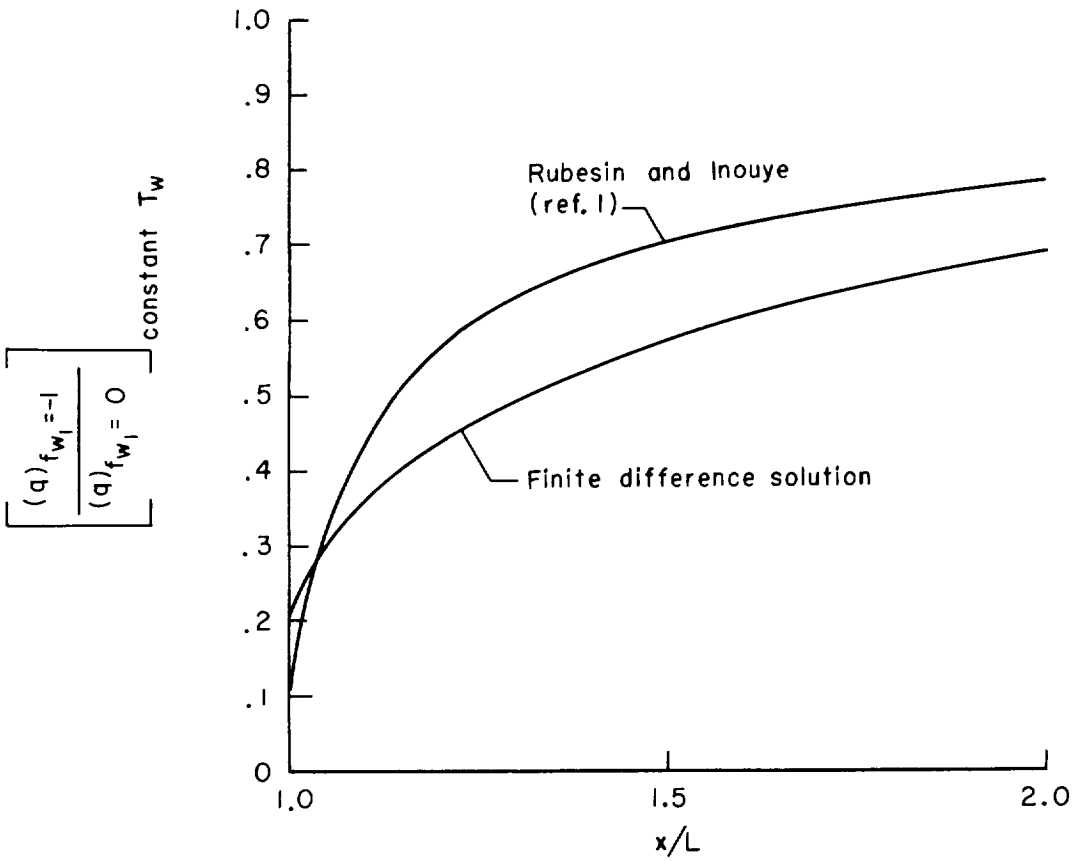

Figure 9.- Comparison of heat-transfer ratio results (ratio of local heat transfer with to that without upstream transpiration cooling at fixed flight temperature and wall temperature); M_e=3.0, T_w=452.34° R, tropopause flight temperature.

NASA MEMO 2-26-59A
National Aeronautics and Space Administration.
SOME FINITE DIFFERENCE SOLUTIONS OF THE LAMINAR COMPRESSIBLE BOUNDARY LAYER SHOWING THE EFFECTS OF UPSTREAM TRANSPIRATION COOLING. John T. Howe. February 1959. 33p. diagrs., tabs.
(NASA MEMORANDUM 2-26-59A)

Three numerical solutions of the partial differential equations describing the compressible laminar boundary layer are obtained by the finite difference method described in reports by I. Flügge-Lotz, D. C. Baxter, and this author. The solutions apply to steady-state supersonic flow without pressure gradient over a cold wall and over an adiabatic wall both having transpiration cooling upstream, and over an adiabatic wall with upstream cooling, but without upstream transpiration. The results of the numerical solutions are compared with those of approximate methods.

Copies obtainable from NASA, Washington

1. Flow, Supersonic (1.1.2.3)
2. Flow, Laminar (1.1.3.1)
3. Heat Transfer, Aerodynamic (1.1.4.2)
4. Boundary-Layer Characteristics - Wing Sections (1.2.1.6.1)
5. Heat Transfer (3.9)
I. Howe, John T.
II. NASA MEMO 2-26-59A

NASA

NASA MEMO 2-26-59A
National Aeronautics and Space Administration.
SOME FINITE DIFFERENCE SOLUTIONS OF THE LAMINAR COMPRESSIBLE BOUNDARY LAYER SHOWING THE EFFECTS OF UPSTREAM TRANSPIRATION COOLING. John T. Howe. February 1959. 33p. diagrs., tabs.
(NASA MEMORANDUM 2-26-59A)

Three numerical solutions of the partial differential equations describing the compressible laminar boundary layer are obtained by the finite difference method described in reports by I. Flügge-Lotz, D. C. Baxter, and this author. The solutions apply to steady-state supersonic flow without pressure gradient over a cold wall and over an adiabatic wall both having transpiration cooling upstream, and over an adiabatic wall with upstream cooling, but without upstream transpiration. The results of the numerical solutions are compared with those of approximate methods.

Copies obtainable from NASA, Washington

1. Flow, Supersonic (1.1.2.3)
2. Flow, Laminar (1.1.3.1)
3. Heat Transfer, Aerodynamic (1.1.4.2)
4. Boundary-Layer Characteristics - Wing Sections (1.2.1.6.1)
5. Heat Transfer (3.9)
I. Howe, John T.
II. NASA MEMO 2-26-59A

NASA

NASA MEMO 2-26-59A
National Aeronautics and Space Administration.
SOME FINITE DIFFERENCE SOLUTIONS OF THE LAMINAR COMPRESSIBLE BOUNDARY LAYER SHOWING THE EFFECTS OF UPSTREAM TRANSPIRATION COOLING. John T. Howe. February 1959. 33p. diagrs., tabs.
(NASA MEMORANDUM 2-26-59A)

Three numerical solutions of the partial differential equations describing the compressible laminar boundary layer are obtained by the finite difference method described in reports by I. Flügge-Lotz, D. C. Baxter, and this author. The solutions apply to steady-state supersonic flow without pressure gradient over a cold wall and over an adiabatic wall both having transpiration cooling upstream, and over an adiabatic wall with upstream cooling, but without upstream transpiration. The results of the numerical solutions are compared with those of approximate methods.

Copies obtainable from NASA, Washington

1. Flow, Supersonic (1.1.2.3)
2. Flow, Laminar (1.1.3.1)
3. Heat Transfer, Aerodynamic (1.1.4.2)
4. Boundary-Layer Characteristics - Wing Sections (1.2.1.6.1)
5. Heat Transfer (3.9)
I. Howe, John T.
II. NASA MEMO 2-26-59A

NASA

NASA MEMO 2-26-59A
National Aeronautics and Space Administration.
SOME FINITE DIFFERENCE SOLUTIONS OF THE LAMINAR COMPRESSIBLE BOUNDARY LAYER SHOWING THE EFFECTS OF UPSTREAM TRANSPIRATION COOLING. John T. Howe. February 1959. 33p. diagrs., tabs.
(NASA MEMORANDUM 2-26-59A)

Three numerical solutions of the partial differential equations describing the compressible laminar boundary layer are obtained by the finite difference method described in reports by I. Flügge-Lotz, D. C. Baxter, and this author. The solutions apply to steady-state supersonic flow without pressure gradient over a cold wall and over an adiabatic wall both having transpiration cooling upstream, and over an adiabatic wall with upstream cooling, but without upstream transpiration. The results of the numerical solutions are compared with those of approximate methods.

Copies obtainable from NASA, Washington

1. Flow, Supersonic (1.1.2.3)
2. Flow, Laminar (1.1.3.1)
3. Heat Transfer, Aerodynamic (1.1.4.2)
4. Boundary-Layer Characteristics - Wing Sections (1.2.1.6.1)
5. Heat Transfer (3.9)
I. Howe, John T.
II. NASA MEMO 2-26-59A

NASA